Article

A Fluorogenic Molecule to Probe Islet Amyloid Using Flavonoid as a Scaffold Design

Wei-Ling Chen, Shih-Ting Ma, Yun-Wen Chen, Yen-Cheng Chao, Ai-Ci Chan, Ling-Hsien Tu, and Wei-Min Liu

Biochemistry, **Just Accepted Manuscript** • DOI: 10.1021/acs.biochem.0c00076 • Publication Date (Web): 08 Apr 2020

A Fluorogenic Molecule to Probe Islet Amyloid Using Flavonoid as a Scaffold Design

Wei-Ling Chen[1,†], Shih-Ting Ma[2,†], Yun-Wen Chen[3], Yen-Cheng Chao[2], Ai-Ci Chan[1], Ling-Hsien Tu[1*] and Wei-Min Liu[2*]

1. Department of Chemistry, National Taiwan Normal University, Taipei 116, Taiwan.
2. Department of Chemistry, Fu Jen Catholic University, New Taipei City 24205, Taiwan.
3. Department of Pharmacology, College of Medicine, National Cheng Kung University, Tainan 701, Taiwan.

† These authors contributed equally

* To whom correspondence should be addressed: Ling-Hsien Tu, E-mail: litu@ntnu.edu.tw; Wei-Min Liu, E-mail: 133797@mail.fju.edu.tw

Abstract

Aggregation of polypeptides and proteins is commonly associated with human and other vertebrate diseases. For example, amyloid plaques consist of amyloid-β proteins (Aβ) are frequently identified in Alzheimer's disease and islet amyloid formed by islet amyloid polypeptide (IAPP, Amylin) can be found in most patients with type-2 diabetes (T2D). Although many fluorescent dyes have been developed to stain amyloid fibrils, very few examples are designed for IAPP. In this study, a series of environmentally sensitive fluorescent probes using flavonoid as a scaffold design is rationally designed and synthesized. One of these probes, namely 3-HF-ene-4'-OMe, can bind to IAPP fibrils but not non-fibrillar IAPP by exhibiting a much stronger fluorescent enhancement at 535 nm. In addition, this probe shows better detection sensitivity to IAPP fibrils compared with conventionally used Thioflavin-T. We demonstrate that 3-HF-ene-4'-OMe can be used to monitor the kinetics of IAPP fibril formation *in vitro* even in the presence amyloid inhibitor. To test the specificity of probe, we attempt to incubate this probe with amyloid fibrils formed from other amyloidogenic proteins. Interestingly, this probe shows different responses when mixing with these fibrils suggesting the binding mode of this probe on these fibrils could be different. Moreover, we show that this probe is not toxic to pancreatic mouse beta cells. Further structural optimization based on the structure of 3-HF-ene-4'-OMe may accomplish a specific probe for imaging islet amyloid in the pancreas. That would improve our understanding on the relationship between islet amyloid and T2D.

Introduction

The self-assembly of amyloidogenic proteins or peptides plays a crucial role in many human diseases such as Parkinson's disease, Alzheimer's disease (AD), and type-2 diabetes (T2D)[1, 2]. Although these proteins are different in sequence and length, under incompletely defined circumstance, they would misfold, associate into typical β-sheet conformation, and form characteristic aggregated oligomers or fibrils. The mechanism of amyloid formation has not been fully elucidated, however, many studies have suggested that the occurrence of fibril formation is frequently associated with the rate of disease onset. Consequently, tons of efforts were consistently made by scientists to reveal the mechanism of protein aggregation, to design methods for preventing protein aggregation, and to develop better probes for detecting protein aggregation.

Thioflavin-T (ThT) is the most commonly used fluorescent probe for detecting fibril growth kinetics *in vitro*[3, 4]. However, there are several drawbacks and cautions should be taken when using ThT as an amyloid probe. For example, the non-specific binding of ThT to other hydrophobic patches sometimes results in a false positive signal[5, 6]. The binding affinity of ThT to amyloid fibrils varies significantly and that is highly dependent on the pH and the ionic strength[7] of working solution. An excess of ThT, relative to amyloid fibrils, is generally required to achieve high fluorescence enhancement[8]. As a result, the ThT assay does not always accurately report the presence of amyloid fibrils. Furthermore, it may not always be reliable using ThT for inhibition studies, because some potential inhibitory candidates compete with ThT for the same amyloid binding site or quench ThT fluorescence resulting prejudiced conclusions[9-11]. Therefore, the development of efficient and specific fluorescent probes is necessary and the use of multiple dyes in drug screening is needful. Recently, although many specific fluorescent probes have been reported for different neurodegenerative amyloidosis [11-18], there are very few examples designed in particular for islet amyloid polypeptide (IAPP)[19-21]. IAPP is a 37-residue hormone polypeptide with a disulfide bridge between Cys-2 and Cys-7 (Figure 1A) and co-secreted with insulin from pancreatic β-cells. The aggregation process of IAPP has been shown to cause the loss of β-cells [22]. Accumulation of islet amyloid in the pancreas also has become one of the important features of T2D[23-25]. Therefore, it is believed that the development of specific dye for the detection of islet amyloid would enhance our understanding of this disease and help us find useful inhibitors against islet amyloid aggregation.

Flavonoids are a class of natural products which are capable of disrupting aggregation of amyloidogenic proteins[26, 27]. For instance, epigallocatechin gallate (EGCG) and silibinin sharing a similar flavonoid like core structure (Figure 1B) were found to efficiently prevent aggregation of IAPP[28]. On the other hand, it is also worth noting that flavonoid-based small molecules, 3-hydroxyflavone (**3-HF**) and its

derivatives, are environmentally sensitive (solvatochromic) fluorescent dyes with characteristic separated dual emission bands[29]. The dual-band emissions are due to intramolecular proton transfer (ESIPT) in the excited state and that produces two excited state forms, namely normal state (N^*, excited state intramolecular charge transfer, ESICT product) and tautomer state (T^*, ESIPT product). In comparison with N^*, the T^* results in a longer wavelengths emission and that can be easily modulated by dipolar and H-bonding interaction[30]. The ratio of the intensities of these two bands highly depends on the polarity of the environment[31]. Because of these unique features, **3-HF** and its derivatives have been widely applied in the studies of polymers[32], reverse micelles[33], and proteins[34-36]. Along these lines, flavonoid was considered as an ideal scaffold for the design of our fluorescent probes. Besides, the conjugated 4'-methoxybenzene motif of stilbene derivative is another well-known molecular skeleton with high binding affinity for amyloid fibrils[37]. In order to optimize the binding affinity of our probes to IAPP fibrils, different length of conjugated π-electron chain was employed. Thus, a series of environmentally sensitive fluorescent probes was rationally designed and synthesized (Figure 1B). Herein, one of these probes, namely **3-HF-ene-4'-OMe**, exhibits better detection properties for IAPP amyloid, acts as an alternative fluorescent dye in the studies of IAPP aggregation kinetics *in vitro*, and is also suitable for IAPP inhibitory studies. **3-HF-ene-4'-OMe** displays unique maximum emission wavelength at 535 nm upon binding to IAPP fibrils but not to non-fibrillar IAPP or other amyloid fibrils suggesting its potential to be developed as a specific dye. In this

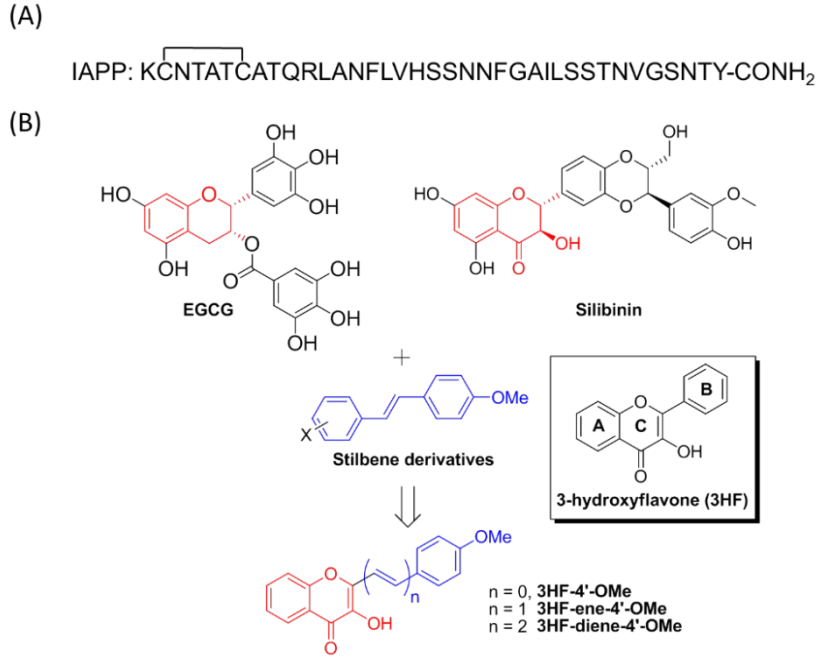

Figure 1. (A) The amino acid sequences of IAPP. IAPP is amidated at C-terminal and contains a disulphide bond between residue 2 and 7. (B) Design of environmentally sensitive fluorescent probes for detecting IAPP amyloid fibrils.

study, we chose amyloid fibrils formed by amyloid beta ($A\beta_{42}$) and human calcitonin (hCT) for comparison with IAPP fibrils. Deposition of amyloid plaques composed of Aβ in the brain is highly associated with Alzheimer's disease. hCT is also a member of amylin protein family. These two peptides are both considered as amyloidogenic peptides. Additionally, we also demonstrate that non-cytotoxic **3-HF-ene-4'-OMe** can be applied in live cells imaging. However, further structural optimization based on **3-HF-ene-4'-OMe** is needed to improve its nonspecific binding to cell membrane. The probe holds promising potential for imaging of islet amyloids in the pancreas.

Materials and Methods

General protocol for the synthesis of a series of flavonoid-based probes.

To a solution of 2'-hydroxyacetophenone (1 equiv.) and corresponding aldehydes **1a-1c** (1 equiv.) in MeOH was added 15 M NaOH under ice bath. The reaction mixture was stirred at room temperature until no aldehyde remained, checking by TLC. Until the reaction was complete, solution was acidified by concentrated HCl (37%) until pH 1 ~ 2. The acidified reaction solution was filtered through Büchner funnel. The filter cake was directly used for the next step or was purified by recrystallization using EtOAc as solvent. The products from previous step were dissolved in MeOH, then NaOH (5 equiv.) and H_2O_2 (25 equiv.) were added into the reaction mixture at 0 °C. The reaction mixture was allowed to stir at room temperature for 24 hr. After that, it was diluted with ice water and 4N HCl aqueous solution was added to adjust the pH until 1. The resulting precipitates were filtered and washed with distilled water, giving the desired products or was further purified by crystallization or purified by flash column chromatography, giving the desired products. **3-HF-4'-OMe** (Yield: 73%): ^{1}H NMR (300 MHz, d_6-DMSO, 294 K): δ = 9.47 (s, OH), 8.30 (d, J = 9.0 Hz, 2H, $H_{2'}$, $H_{6'}$), 8.07 (dd, J_1 = 7.6 Hz, J_2 = 1.0 Hz, 1H, H_5), 7.75-7.68 (m, 2H, H_7, H_8), 7.40 (ddd, J_1 = 8.0 Hz, J_2 = 5.9 Hz, J_3 = 2.1 Hz, 1H, H_6), 7.08 (d, J = 9.1 Hz, 2H, $H_{3'}$, $H_{5'}$), 3.82 (s, 3H, OMe) ppm; ^{13}C NMR (75 MHz, d_6-DMSO, 298 K): δ = 172.61, 160.43,154.42, 138.13, 133.47, 129.39, 124.71, 124.46, 123.56, 121.33, 118.30, 114.03, 55.35 ppm; IR (KBr): 3198, 3018, 2837, 1633, 1614, 1483, 1308, 1132, 1111, 1025, 830, 757 cm^{-1}; The data agreed with literature reported[38]. **3-HF-ene-4'-OMe** (Yield: 46%): R_f = 0.2 (n-Hexane: EtOAc 7:1 v/v). ^{1}H NMR (300 MHz, $CDCl_3$, 295 K): δ = 8.22 (dd, J_1 = 8.0 Hz, J_2 = 1.6 Hz, 1H, H_5), 7.71 (ddd, J_1 = 8.6 Hz, J_2 = 7.1 Hz, J_3 = 1.7 Hz, 1H, H_7), 7.60-7.49 (m, 4H, $H_{2'}$, $H_{6'}$, H_8, H_β), 7.39 (ddd, J_1 = J_2 = 7.5 Hz, J_3 = 1.0 Hz, 1H, H_6), 7.21 (d, J = 16.2 Hz, 1H, H_α), 6.95 (d, J = 8.8 Hz, 2H, $H_{3'}$, $H_{5'}$), 3.86 (s, 3H, OMe) ppm; ^{13}C NMR (75 MHz, $CDCl_3$, 300 K): δ = 172.50, 160.84, 155.23, 146.05, 137.57, 134.36, 133.47, 129.23, 128.87, 125.52, 124.42, 121.56, 118.17, 114.54, 113.60, 55.55 ppm; IR (KBr): 3117, 1636, 1617, 1469, 1304, 1255, 1170, 1114, 1024, 963, 818, 800, 757 cm^{-1}; m.p. = 229-

230 °C; HR-MS m/z: 295.0970 $[M+H]^+$, calcd. $[C_{18}H_{15}O_4]$: 295.0970.; **3-HF-diene-4'-OMe** (Yield: 55%): R_f = 0.17 ($CHCl_3$). ^1H NMR (600 MHz, d_6-DMSO, 300 K): δ = 9.50 (s, OH), 8.05 (dd, J_1 = 8.0 Hz, J_2 = 1.6 Hz, 1H, H_5), 7.76 (ddd, J_1 = 8.6 Hz, J_2 = 7.1 Hz, J_3 = 1.7 Hz, 1H, H_7), 7.65 (d, J = 8.4 Hz, 1H, H_8), 7.53 (d, J = 8.8 Hz, 2H, $H_{2'}$,$H_{6'}$), 7.43 (ddd, J_1 = 7.5 Hz, J_2 = 7.5 Hz, J_3 = 0.9 Hz, 1H, H_6), 7.35 (dd, J_1 = 15.1Hz, J_2 = 10.8 Hz, 1H, H_β), 7.12 (dd, J_1 = 15.3 Hz, J_2 = 11.0 Hz, 1H, H_γ), 6.86 (d, J = 9.0 Hz, 2H, $H_{3'}$, $H_{5'}$), 6.85 (d, J = 15.0 Hz, 1H, H_δ), 6.82 (d, J = 15.0 Hz, 1H, H_α), 3.78 (s, 3H, OMe) ppm; ^{13}C NMR (150 MHz, d_6-DMSO, 300 K): δ = 172.00, 159.88, 154.35, 146.93, 138.02, 137.11, 135.07, 133.76, 129.47, 128.69, 126.32, 124.96, 124.58, 122.24, 118.48, 118.21, 114.57, 55.45 ppm; IR (KBr) = 3189, 1614, 1590, 1469, 1302, 1260, 1172, 1153, 1114, 1062, 1027, 985, 837, 760 cm^{-1}; m.p. = 226-229 °C; HR-MS m/z: 321.1129 $[M+H]^+$, calcd. $[C_{20}H_{17}O_4]$: 321.1127. The details of peak assignments of 1H NMR spectra are also shown in supporting information.

Peptide synthesis

IAPP, $A\beta_{42}$, and hCT were synthesized with standard Fmoc solid phase synthesis using a microwave-assisted CEM Liberty Lite peptide synthesizer. In order to generate amidated C-terminus, Rink amide ProTide resin as solid phase support was used for IAPP and hCT synthesis. Fmoc-protected pseudoproline dipeptides were used to avoid peptide aggregation during IAPP synthesis. For $A\beta_{42}$, Cl-MPA ProTide resin was used and a 1.0 M *N*, *N*-diisopropylethylamine (DIEA) and 0.125 M KI solution were prepared for first amino acid coupling. After synthesis, peptides were cleaved from the resin by using a cocktail containing 92.5% trifluoroacetic acid (TFA), 2.5% water, 2.5% 3,6-dioxa-1,8-octanedithiol (DODT), and 2.5% triisopropylsilane (TIS). Crude IAPP and hCT were oxidized with CLEAR-OX resin at room temperature to form an intramolecular disulfide bond. All peptides were purified via reverse-phase high-performance liquid chromatography (HPLC) using PROTO C18 semi-preparative column (4.6 mm x 250 mm). A two solution gradient system was used for IAPP and hCT purification: solution A consisted of 100% H_2O and 0.045% HCl (v/v) and solution B consisted of 80% acetonitrile (ACN), 20% H_2O and 0.045% HCl. For $A\beta_{42}$ purification, we used another alkalic solution system to increase peptide solubility. Solution A consisted of 100% H_2O, 0.05% NH_4OH and 0.005 % diethylamine (DEA, pH was adjusted to 10 by TFA) and solution B consisted of 90% ACN, 10% H_2O, 0.05% NH_4OH and 0.005 % DIEA (pH was adjusted to 10 by TFA). The molecular weight of IAPP was confirmed by ESI mass spectrometry. ESI (positive mode) calcd. for IAPP: 3903.3, found: m/z 976.7 $[M+4H]^{4+}$ and 1302.3 $[M+3H]^{3+}$. MALDI-TOF mass spectrometry confirmed the molecular weight of $A\beta_{42}$ (expected, 4514.1 Da; observed, 4514.5 Da) and hCT (expected, 3417.8 Da; observed, 3418.6 Da).

Sample preparations

Small molecules, **3-HF**, **3-HF-4'-OMe**, **3-HF-ene-4'-OMe** and **3-HF-diene-4'-OMe** were first prepared in pure dimethyl sulfoxide (DMSO) at 32 mM and diluted into 10 mM Tris buffer at pH 7.4 to make a concentration of 32 or 64 μM solution. Absorption spectra were collected using SpectraMax M2 multimode plate reader. Excitation and emission wavelengths for individual compound were determined and shown in supporting information (Figure S2). The environmental sensitivity of these probes was studied with a DMSO and water cosolvent system (Figure S1D-F). To prepare non-fibrillar peptide and peptide fibrils, all peptides were first treated with 1,1,1,3,3,3-hexafluoro-2-propanol (HFIP) to disassembly possible aggregates and freeze-dried by lyophilizer. 0.1~0.2 mg dry power peptides were dissolved in 100 μL, 10 mM Tris buffer at pH 7.4 and Pierce BCA protein assay kit (BSA as protein standard, Thermo Scientific) was used to determine peptide concentration. Then peptide stock was further diluted to the desired concentrations. Non-fibrillar peptide solution was always fresh prepared before measurements. To prepare fibril solutions, peptides were further incubated at 25 ^{o}C for 2.5 days with continuous shaking (Eppendorf, ThermoMixer C). Formation of amyloid fibrils was confirmed by ThT assay and TEM.

Fluoresce spectra of 3-HF and its derivatives with non-fibrillar peptide and peptide fibrils

Both non-fibrillar peptide solution and fibril solution were prepared at 64 μM determined by BCA assay. Then individual compound DMSO solution was added into non-fibrillar peptide or fibril solution to reach a final concentration of 64 μM and DMSO concentration was fixed in 1%. The well-mixed solution was excited at different wavelengths according to different maximal absorption of compounds, and emission spectra were recorded for a wide range.

Circular dichroism (CD)

CD experiments were performed using a JASCO J-715 circular dichroism spectrometer. In order to avoid the interference of DMSO, we first prepared the probe in acetonitrile (ACN)[39]. The final concentration of ACN in IAPP solution is 1%. CD experiments were conducted after incubation of 64 μM IAPP solution with and without the probe at 25 ^{o}C for 3 days with continuous shaking. Spectra were recorded from 200 to 260 at 1 nm intervals at 25 °C. The data were averaged from ten scans and corrected with background spectrum.

Determination of fluorescence enhancement of ThT and 3-HF-ene-4'-OMe for IAPP fibrils

The fluorescence of ThT (λ_{em} = 485 nm) and **3-HF-ene-4'-OMe** (λ_{em} = 535 nm) are recorded when increasing concentration (0-64 μM) of probes were titrated into fixed IAPP fibrils (64 μM). The half maximal concentration C_M were analyzed by Graph Pad Prism 5.0 using the equation Y= Bmax*X/(C_M+ X) where X is the concentration of

probes, Y is the change of fluorescence intensity, Bmax is the maximum binding of probes with the same units as Y, and C_M is half maximal concentration with the same units as X.

ThT and 3-HF-ene-4'-OMe aggregation assay

Aliquot of freshly prepared IAPP stock was diluted into buffer containing 32 μM ThT (from a 1 mM ThT solution) or 32 μM **3-HF-ene-4'-OMe** to make a concentration of 32 μM solution. A 384-well nonbinding surface microplate (Corning, USA) was used for ThT measurement. ThT fluorescence was excited at 430 nm and collected at 485 nm while **3-HF-ene-4'-OMe** fluorescence was excited at 380 nm and collected at 535 nm using SpectraMax M2 multimode plate reader under quiescent conditions. The measurement was conducted every two hours. For resveratrol inhibition studies, resveratrol was first prepared in DMSO and then added into IAPP with ThT or IAPP with **3-HF-ene-4'-OMe** solution to reach desired concentration. The total concentration of DMSO was fixed in less than 2%.

TEM

5 μL of IAPP, $A\beta_{42}$, hCT samples were deposited onto 300-mesh Formvar carbon-coated copper grids for 1 min. The grids were blotted, washed with droplets of Milli-Q water, and stained with 2% uranyl acetate. The samples were examined with Hitachi H-7100 transmission electron microscopy with an accelerating voltage of 120 kV.

Molecular docking

3-HF-ene-4'-OMe docking studies with IAPP and $A\beta_{42}$ fibrils were executed by using Autodock 4.2 software package[40]. The structure of $A\beta_{42}$ fibrils (PDB: 2MXU)[41] was download from the Protein Data Bank and the model of IAPP fibrils was provided by Prof. Robert Tycko[42] and modified by Prof. Daniel P. Raleigh. The geometry of **3-HF-ene-4'-OMe** in the gas phase was optimized with density functional theory at the B3LYP/6-31G* level using Gaussian09 program[43, 44]. The docking simulations were carried out with a box centered on the IAPP fibrils and a box centered on the $A\beta_{42}$ fibrils. The sizes of the boxes are 126 × 126 × 126 Å using a 0.375 Å grid step for both IAPP and $A\beta_{42}$ fibrils. The docking simulation was performed 100 times and the Lamarckian Genetic Algorithm was employed for the grid search algorithm.

Confocal fluorescence imaging

For the confocal image observation, IAPP amyloid fibrils were prepared at 32 μM and mixed with 32 μM **3-HF-ene-4'-OMe** in 10 mM Tris buffer (pH 7.4). The mixed solutions were placed onto a glass slide. Confocal images were taken with a laser scanning confocal microscope (Leica SP5). **3-HF-ene-4'-OMe** was excited with an Ar-ion laser at 380 nm, and detected in the range of 500-580 nm. Transmitted light images was also obtained to assess the presence of fibrils in the investigated region.

Cell culture

Murine insulin-secreting MIN6 cells were grown in Dulbecco's Modified Eagle's Medium (DMEM; Gibco) supplemented with 25 mM glucose, 10% heat-inactivated fetal bovine serum (FBS; Gibco), 100 U/ml penicillin, 100 μg/ml streptomycin (Gibco), 10 mM HEPEs (Gibco), 1 mM sodium pyruvate (Gibco) and 2 mM GlutaMax (Gibco). Cells were cultured at 37 °C in a humidified atmosphere containing 95% air and 5% CO_2. Subculture and maintenance were performed as previously described[45]. Cultured cells were passaged every 3–4 days. MIN6 cells presented in this study were at passages 20–30.

Fluorescence imaging

MIN6 Cells were seeded on the glass-bottom dish (1×10^5 cells) for three days. To examine the binding ability of **3-HF-ene-4'-OMe** for IAPP fibrils in live cells, MIN6 cells were incubated with 8 μM IAPP fibrils for 1 hr, and then incubated with **3-HF-ene-4'-OMe** for 2 hr in the growth medium. After that, cells were washed with PBS buffer for three times prior to fluorescence imaging. The images were taken by Fluorescence microscopy.

Cell viability assay

MIN6 Cells were seeded in 96 well plates (8×10^4 cells/well) and cultured for three days before exposure to IAPP probe (24 hr, 48 hr, 72 hr) and then the 3-(4,5-diethylthiazol-2-yl)-2,5-diphenyltetrazolium bromide (MTT) assay was used to assess the viability of cells after IAPP probe treatment.

Results and Discussion

Before introduction of our probes in the test, the preparation of IAPP fibrils was further confirmed by traditional ThT assay and transmission electron microscopy (TEM, Figure 2A and Figure S1). It was shown that ThT with IAPP fibrils exhibited stronger fluorescence in comparison with freshly prepared IAPP. TEM also showed the typical fibrillar structure of amyloid. In this study, **3-HF** was initially used to evaluate the ability of flavonoid scaffold for the detection of amyloid fibrils. As shown in Figure 2B, the fluorescence intensity of **3-HF** was dramatically increased upon addition to IAPP fibrils, although a similar result was observed when **3-HF** was mixed with non-

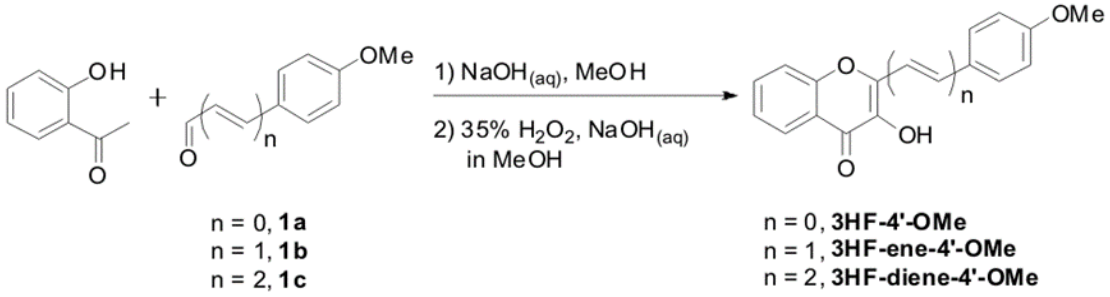

Scheme 1. The synthesis of **3-HF-4'-OMe**, **3-HF-ene-4'-OMe**, and **3-HF-diene-4'-OMe**.

fibrillar IAPP which is considered a very hydrophobic peptide. Encouraged by this preliminary outcome, the B ring of **3-HF** was functionalized with a methoxy group at para-position to mimic the structure of stilbene derivatives. Different length of conjugated π-electron chains was created between ring C and ring B of **3-HF** and to improve the fibril selectivity. The synthesis of a series of flavonoid-based probes is shown in Scheme 1. Aldehyde **1c** was prepared from **1b** according to the reported procedure (supporting information)[46]. When the appropriate aldehydes were prepared, they were condensed with 2'-hydroxyacetophenone to produce the conjugated diphenyl intermediates. Subsequently, Algar-Flynn-Oyamada reaction was applied to make desired fluorescent probes[38, 47].

First, the UV and fluorescence spectrum for synthetic flavonoid-based probes were measured. The excitation/maximum emission wavelength of **3-HF-4'-OMe**, **3-HF-ene-4'-OMe**, and **3-HF-diene-4'-OMe** in dimethyl sulfoxide (DMSO) were 355/555, 390/475, and 415/545 nm, respectively. Next, the environmental sensitivity of these probes was evaluated to confirm that these molecules are solvatochromic (Figure S2). As anticipated, dual fluorescence emissions of **3-HF-4'-OMe** were found and the ratio of these two fluorescence peak intensities was strongly depended on the

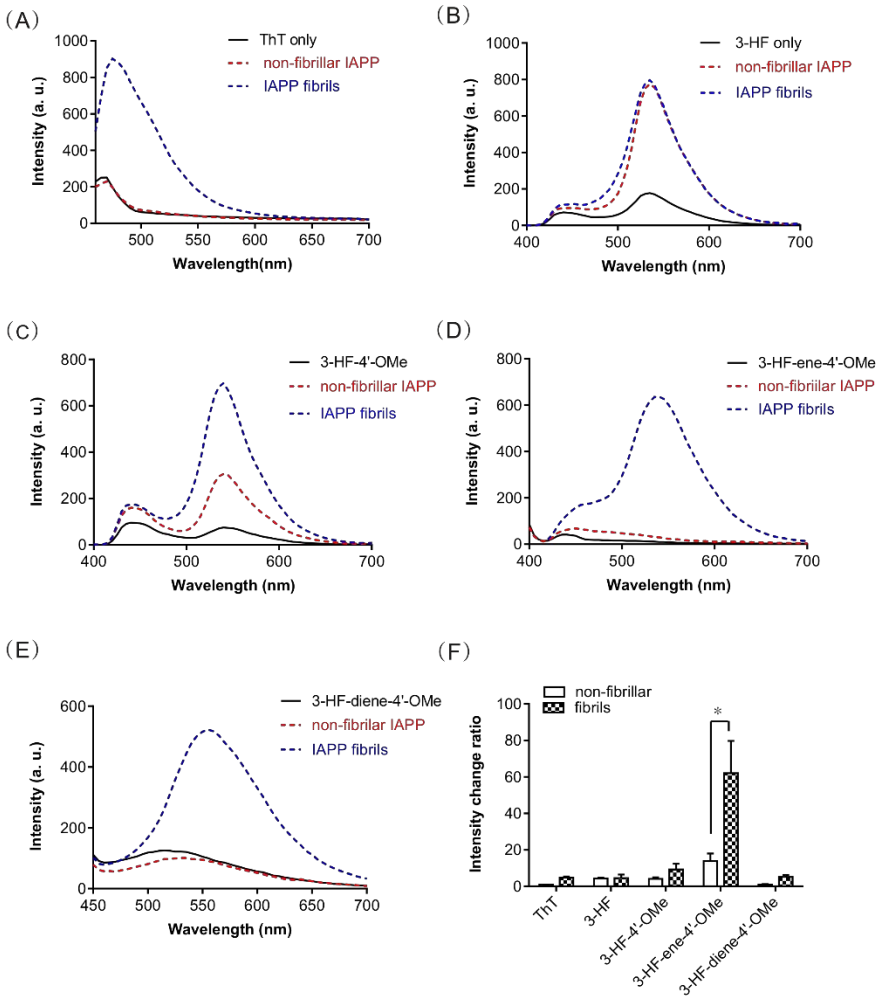

Figure 2. **3-HF-ene-4'-OMe** is the most sensitive dye to distinguishing non-fibillar IAPP and IAPP fibrils. Fluorescence emission spectra of (A) ThT, (B) **3-HF**, (C) **3-HF-4'-OMe**, (D) **3-HF-ene-4'-OMe**, and (E) **3-HF-diene-4'-OMe** at 64 μM are measured. Black curve represents probe alone. Red dot curve represents probe with non-fibillar IAPP. Blue dot curve represents probe with IAPP fibrils. All measuremnets were performed in 10 mM Tris buffer at pH 7.4 in duplicate. The IAPP fibrils were prepared by incubation of samples in microtubes for 2.5 days with continuous shaking. (F) The ratio of fluorescence increase of flavonoid-based probes and ThT mixed with non-fibillar IAPP or fibrils relative to the fluorescence intensity of free probes in 10 mM Tris buffer at pH 7.4. (Wavelenths were used for claculation. ThT: 485 nm; 3-HF: 535 nm; 3-HF-4'-OMe: 540 nm; 3-HF-ene-4'-OMe: 535 nm; 3-HF-diene-4'-OMe: 555 nm)

water concentration in DMSO (Figure S2D). Instead of dual emission bands, **3-HF-ene-4'-OMe** and **3-HF-diene-4'-OMe** display a single broad emission band. The broadening emission band could result from the increase of the flexibility of conjugated double bonds (Figure S2E and F). Despite they both exhibit a single broad emission band, the fluorescence intensity and maximal emission wavelength of these two probes still strongly depend on the environmental polarity and viscosity. **3-HF-ene-4'-OMe** and **3-HF-diene-4'-OMe** exhibit a significant red-shift about 70 nm and 40 nm, respectively, when the percentage of water in solution increases from 0% to 40% (Figure S2E and F). Fluorescence of these two probes enhance along with increasing viscosity (Figure S2G and H). Meanwhile, all of these flavonoid-based probes display negligible fluorescence emission in aqueous solution (Figure S2C). After understanding the optical properties of these probes, we next examined their ability in detecting preformed IAPP fibrils. As shown in Figure 2, in all cases, the fluorescence intensities of these probes significantly increased when they were incubated with IAPP fibrils. In particular, **3-HF-ene-4'-OMe** was found to be the most sensitive dye in differentiating non-fibrillar or aggregated IAPP. Basically, this dye exhibits negligible fluorescence in aqueous solution and mixed with non-fibrillar IAPP, yet its fluorescent property was turned on upon mixing with IAPP fibrils. The intensity enhancement ratio of fibril to non-fibrillar species is significantly different ($p<0.001$, Figure 2F, intensity from dye alone was used as individual background). The ratio of dual emission bands (T*/N*) of **3-HF-4'-OMe** was also significantly different when it was mixed with IAPP fibrils compared with non-fibrillar IAPP and free probe in solution. This change indicates that **3-HF-4'-OMe** binds to the hydrophobic region of IAPP fibrils. As a result, the fluorescent spectra were majorly dominated by ESIPT product of **3-HF-4'-OMe**. Because of the sensitivity of **3-HF-4'-OMe** is still less than **3-HF-ene-4'-OMe**, we chose to use **3-HF-ene-4'-OMe** in the following studies. On the other hand, we also evaluate the specificity of **3-HF-ene-4'-OMe** for detection of amyloid fibrils. Bovine serum albumin (BSA), the relative larger protein with major helix structure was also

incubated with this probe. Only a slight enhancement of fluorescence intensity was observed when **3-HF-ene-4'-OMe** was mixed with BSA, indicating its specificity for fibril detection (Figure S3).

The comparison of fluorescence enhancement from ThT and **3-HF-ene-4'-OMe** with IAPP fibrils was also determined here by *in vitro* saturation binding assay. The fluorescent intensity was recorded for each probe at different concentration with pre-aggregated IAPP fibrils in Tris buffer. The half maximal concentration (C_M) of ThT and **3-HF-ene-4'-OMe** were about 48 μM and 12 μM, respectively (Figure 3). The result indicates that the rational designed **3-HF-ene-4'-OMe** exhibits stronger signal change to IAPP fibrils than the generally used ThT although it seems to have minor self-quenching effect when higher concentration of **3-HF-ene-4'-OMe** was applied. As described previously, ThT is a commonly used probe to monitor the kinetics of amyloid formation. Several factors including binding site competition and quenching effect cause this probe not to always report without bias in amyloid inhibition study. Resveratrol, a reported IAPP inhibitor [48-50], is one of the examples [51]. Previous studies have reported that there was no detectable ThT fluorescence intensity when an excess of resveratrol was used for IAPP inhibition studies, even though large amounts of IAPP fibrils were observed by TEM. This phenomena indicates that resveratrol possibly competes with ThT for binding to amyloid fibrils. In this context, **3-HF-ene-4'-OMe** was also examined whether it can be used for both kinetic and inhibition studies. As a useful probe for monitoring the kinetics of fibril formation, the probe itself should not interfere with the fibril formation. To prove that, **3-HF-ene-4'-OMe** along with ThT were incubated with IAPP and the fluorescence of ThT was monitored during the period of IAPP fibril formation. As shown in Figure S4, similar kinetic curves were observed in the presence and absence of **3-HF-ene-4'-OMe** revealing that our probe did not disturb the fibril formation and this probe might have different binding site to IAPP fibrils compared with ThT. We also used CD to show the β-sheet structure of IAPP

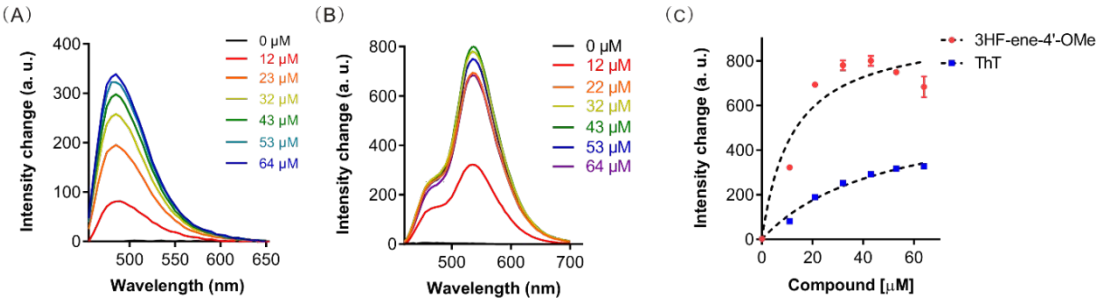

Figure 3. **3-HF-ene-4'-OMe** showed a higher fluorescence signal to islet amyloid than ThT. Fluoresence spectum were recored when (A) ThT and (B) **3-HF-ene-4'-OMe** were titrated into IAPP fibrils. (C) A plot of the fluorescence intensity at λem 485 nm for ThT and at λem 535 nm for **3-HF-ene-4'-OMe** versus the concentration of probes in the presence of IAPP fibrils. Intensity was recored from independent duplicate trials and averaged.

fibrils and this probe did not change the conformation of fibrils (Figure S5). **3-HF-ene-4'-OMe** shares similar core structure with amyloid inhibitors, EGCG and silibinin, but do not inhibit IAPP aggregation. Although the inhibitory mechanism remains unclear for numerous flavonoids, several studies have suggested that the phenolic hydroxyl groups on B ring are important for the effectiveness of these inhibitors. The structure of **3-HF-ene-4'-OMe** is lack of phenolic hydroxyl groups, so this finding may indicate that the core structure of flavonoid could lead the probe interact with IAPP but not block IAPP assembly. In addition, a typical sigmoidal fibril growth curve with three characteristic nucleation (lag phase), elongation, and equilibrium stages (steady phase) was observed when we use **3-HF-ene-4'-OMe** as a probe and it is similar to the one measured by conventional ThT assay (Figure 4a). Even in the condition with performed fibrils as seeds, probe signal still agrees with ThT signal showing the accelerated aggregation (Figure 4b). Our data clearly showed that **3-HF-ene-4'-OMe** could be used as an alternative probe for IAPP aggregation kinetic studies.

We next aim to investigate whether **3-HF-ene-4'-OMe** can be utilized as a dye for resveratrol inhibition studies. Resveratrol is one of the naturally occurring polyphenols mostly present in red wine and grapes. According to previous studies, it was considered as a potential therapeutic drug for several amyloidosis[52]. To IAPP, resveratrol is a moderate inhibitor. It reduces the rate of amyloid formation by IAPP. Studies by using atomic discrete molecular dynamic simulation also suggested that resveratrol binds to IAPP monomers and stabilizes IAPP oligomers to retard IAPP self-association[53]. However, this compound also was shown to interfere with ThT flurosence[40, 51]. In this study, 5 molar equivalents of resveratrol were incubated with IAPP and the kinetics of fibril formation profile was monitored by either ThT or **3-HF-ene-4'-OMe**. As shown in Figure 5A, ThT fluorescence intensity is greatly reduced when resveratrol is present.

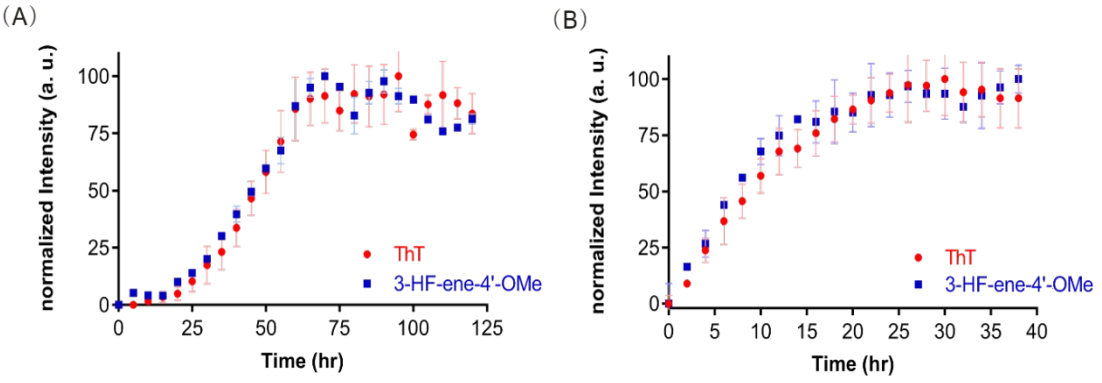

Figure 4. (A) Kinetics of 32 μM IAPP aggregation and (B) kinetics of 32 μM IAPP aggregation with 20% seeds were monitored respectively by 32 μM **3-HF-ene-4'-OMe** (blue) and 32 μM ThT (red) assays. In order to conveniently compare the sigmoidal curves observed from these two assays, each curve was normalized to its individual maximum fluorescence intensity. Reactions in triplicates were performed in 10 mM Tris buffer (pH 7.4) at 25 °C. Seeds were prepared from preformed IAPP fibrils.

Conversely, a clear sigmodal fibril growth curve with an elongated lag phase was observed from **3-HF-ene-4'-OMe** fluorescence suggesting resveratrol did completely inhibit IAPP aggregation, although this final intensity is also reduced. Similar to the previously research[51], large amounts of IAPP fibrils in both samples are observed after incubation for 125 hr (Figure 5B and 5C). The decrease of **3-HF-ene-4'-OMe** fluorescence intensity while mixing with resveratrol may be caused by the interference of resveratrol with **3-HF-ene-4'-OMe** fluorescence, or by the competition between **3-HF-ene-4'-OMe** and resveratrol to the same binding site on IAPP fibrils. To explain the decline of **3-HF-ene-4'-OMe** fluorescence intensity in inhibition study, **3-HF-ene-4'-OMe** in 40% DMSO was first incubated with different amount of resveratrol. The intensity of **3-HF-ene-4'-OMe** retains in the presence of resveratrol indicating that resveratrol does not quench **3-HF-ene-4'-OMe** fluorescence (data not shown). Next, again we monitored IAPP aggregation by **3-HF-ene-4'-OMe** fluorescence. After 96 hr, resveratrol was added into the aggregated sample when fibril formation has achieved a steady phase. The **3-HF-ene-4'-OMe** fluorescence intensity dramatically decreased after the addition of resveratrol, suggesting that the binding of **3-HF-ene-4'-OMe** on IAPP fibrils might be replaced by resveratrol (Figure S6). Although the binding of both ThT and **3-HF-ene-4'-OMe** to IAPP fibrils are interfered by resveratrol, **3-HF-ene-4'-**

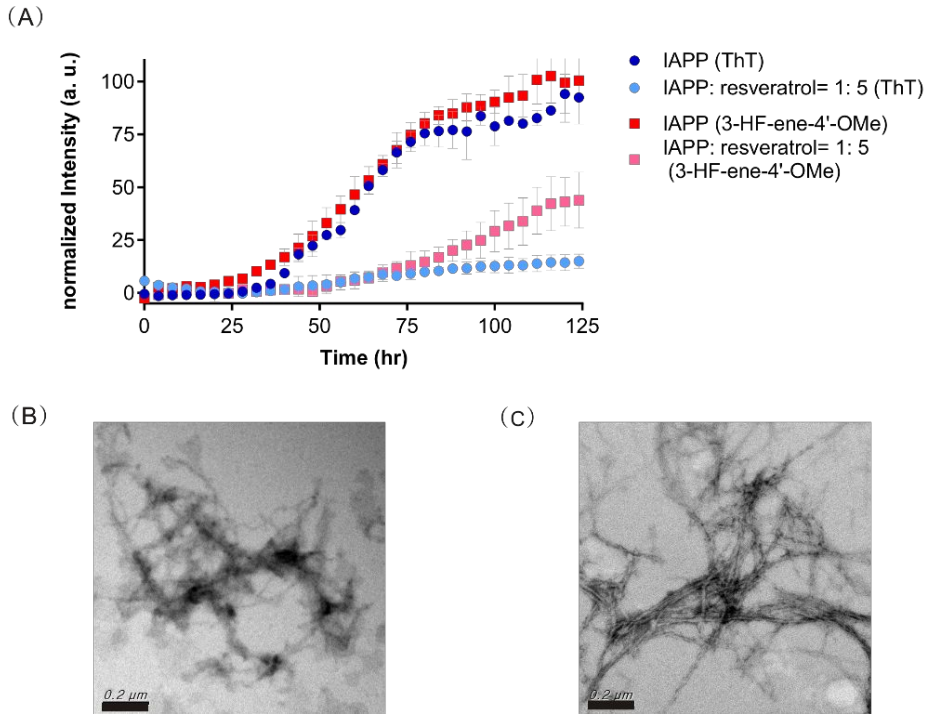

Figure 5. **3-HF-ene-4'-OMe** is suitable to be used in IAPP-Resveratrol inhibition study. (A) The resveratrol inhibitory effect on 32 μM IAPP aggregation was monitored by 32 μM ThT (no inhibitor, blue; with inhibitor, light blue) and 32 μM **3-HF-ene-4'-OMe** (no inhibitor, red; with inhibitor, pink). (B and C) TEM images of IAPP with 5 molar equivalents of resveratrol from ThT assay or **3-HF-ene-4'-OMe** assay after incubation of 125 hr. The scale bar represents 200 nm.

OMe is still more suitable for resveratrol inhibition studies, because a clear sigmoidal curve with elongated lag time was observed when using **3-HF-ene-4'-OMe** as a probe.

To test whether **3-HF-ene-4'-OMe** is specific for detection of IAPP fibrils, other two protein amyloid aggregates formed by $A\beta_{42}$ and hCT were also prepared *in vitro* and the formation of amyloid fibrils was confirmed again by TEM (Figure S7). hCT and IAPP are both belong to amylin protein family. Calcitonin is a 32 amino acid polypeptide, like IAPP, there are two conserved cysteines in the N-terminal and the C-terminal of calcitonin is also amidated. We chose these proteins in our examination because they are similar to IAPP in peptide length and easy to form amyloid fibrils in aqueous solution. Strikingly, the incubation of **3-HF-ene-4'-OMe** with hCT fibrils did not lead to obvious fluorescence enhancement (Figure 6). The fluorescence of **3-HF-ene-4'-OMe** was also lighted on upon binding to $A\beta_{42}$ fibrils, but probe exhibited a weaker signal and a maximum emission wavelength (λ_{max}) which is about 70 nm different to the one detected from IAPP fibrils. Owing to the solubility issue of $A\beta_{42}$ in Tris buffer, the pH value of Tris buffer for Aβ preparation was adjusted to 8.0, which is different from the IAPP sample solution. We speculated that the observed different emission profile could due to the acid-base interactions between amyloid and the probe. To clarify this possibility, **3-HF-ene-4'-OMe** was incubated with IAPP fibrils prepared at the same pH values as $A\beta_{42}$ (Figure S8). Similar emission profile was observed as seen at pH 7.4 and the maximum emission wavelength still falls at 535 nm. The selectivity of **3-HF-ene-4'-OMe** fluorescence emission with IAPP fibrils is not affected by this minor pH change. Different emission profile of **3-HF-ene-4'-OMe** when mixing with aggregated IAPP and $A\beta_{42}$ may due to the difference of the local environment of

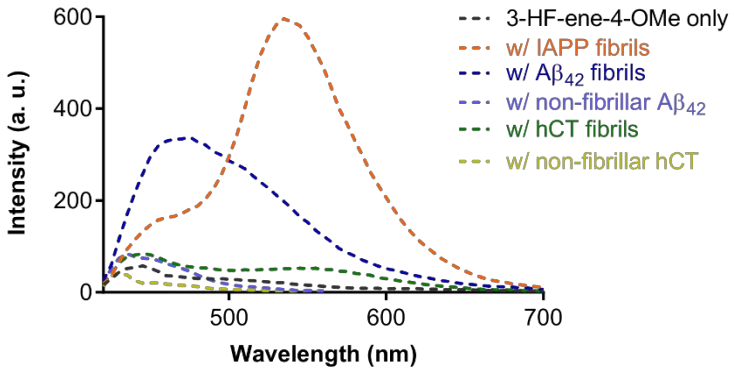

Figure 6. **3-HF-ene-4'-OMe** shows different spectra for three different kinds of amyloid fibrils. Fluorescence emission spectra of **3-HF-ene-4'-OMe** alone (black) and the spectra measured in the presence of IAPP fibrils (orange), $A\beta_{42}$ fibrils (blue), calcitonin fibrils (green), non-fibrillar $A\beta_{42}$ (light blue), and non-fibrillar hCT (yellow). The exiciation wavelength was set at 380 nm. All peptide fibrils were prepared by incubation of peptide samples at 64 μM in microtubes with continuous shaking for 2.5 days at 25 °C. The fibril formation was then further confirmed by ThT and TEM.

this probe in the amyloid binding pocket. **3-HF-ene-4'-OMe** exhibits a shorter emission wavelength when it is in a less polar environment (Figure S2E). Consequently, we deduced that the fluorescence discrimination was due to environmental polarity and the **3-HF-ene-4'-OMe** binding site on $A\beta_{42}$ fibrils is possibly relatively less polar than IAPP fibrils.

In order to assess the binding mode of **3-HF-ene-4'-OMe**, a molecular docking approach was carried out using the most commonly studied IAPP and $A\beta_{42}$ fibril structure model[41, 42]. The results showed that only a single binding site was found when **3-HF-ene-4'-OMe** binds to $A\beta_{42}$ fibrils (Figure 7A and Figure S9). **3-HF-ene-4'-OMe** is clamped inside $A\beta_{42}$ fibrils mainly through π-π stacking interactions with the imidazole ring of His14 and through hydrophobic interaction with Leu17, Leu34, and, Ile32. We speculated this is why **3-HF-ene-4'-OMe** gave a fluorescent emission at lower wavelength, 475 nm, which represents a less polar environment. By contrast, there are multiple binding sites found for **3-HF-ene-4'-OMe** on IAPP fibrils. The binding site with the lowest binding energy is identified inside the IAPP fibrils and the probe would interact with several residues including Gln10, Ala12, Val32, and Ser34 (Figure 7B and Figure S9). However, the most favorable binding site was determined on the IAPP surface around Val17 and Phe15. The water molecules surrounding on the surface of IAPP fibrils can interact with **3-HF-ene-4'-OMe**. This docking result apparently agrees with the observed fluoresce spectrum (Figure 6).

Next, we further examined the potential of **3-HF-ene-4'-OMe** in detection of IAPP fibrils *in vitro* and in live cells. Due to a significant difference in the fluorescence intensity of the free dye and fibrils bound dye, we were able to obtain confocal microscopy images of the **3-HF-ene-4'-OMe** stained fibrillar structures (Figure 8A). From previous studies, it is known that the fluorescent dye containing hydroxyflavone scaffold might be able to bind membrane and increase its quantum yield[54]. Therefore,

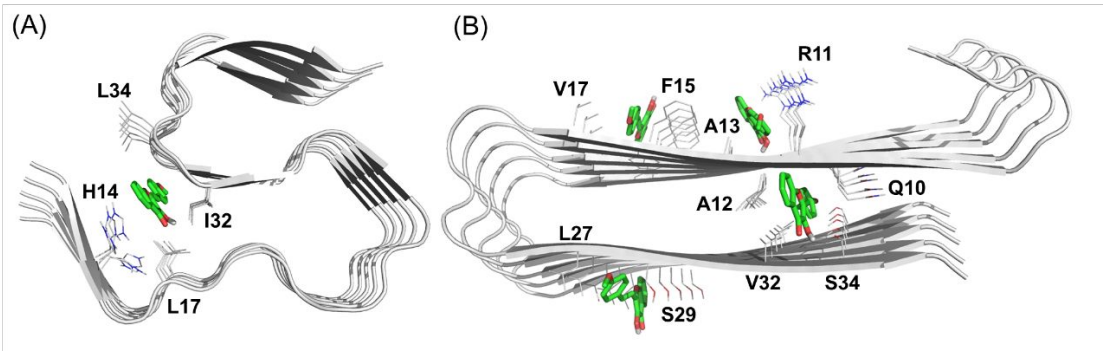

Figure 7. Docking results of **3-HF-ene-4'-OMe** with (A) $A\beta_{42}$ fibrils and (B) IAPP fibrils. The fibrils are shown in cartoon mode and the binding site residues are shown in line with CPK color. **3-HF-ene-4'-OMe** is shown in stick mode and carbon atoms from **3-HF-ene-4'-OMe** are colored in green, oxygen atoms in red and hydrogen atoms from the hydroxyl group in white.

we also used mouse pancreatic beta (MIN6) cells for fluoresce imaging. Mouse pancreatic beta cell did not produce human IAPP, therefore we added preformed IAPP fibrils to cells to mimic the conditions that IAPP formed amyloid outside the beta cells. Before that, MIN6 cells were firstly treated with different concentrations of **3-HF-ene-4'-OMe** for 24 hr, 48 hr, and 72 hr to investigate whether **3-HF-ene-4'-OMe** is cytotoxic. The results showed that there was no significant effect of **3-HF-ene-4'-OMe** on cell viability of MIN6 cells in various concentrations and various incubated times (Figure S10). Thereafter, MIN6 cells were incubated with IAPP fibrils for 1 hr and then stained with **3-HF-ene-4'-OMe**. The fluorescence images revealed that the intensity of green fluorescence with IAPP fibrils was much greater than cells in accompanying with **3-HF-ene-4'-OMe**, suggesting that **3-HF-ene-4'-OMe** could detect IAPP fibrils in live cells (Figure 8B and 8C). Although the probe still has a chance to bind cell membrane then fluoresces, this molecule has shown this potential in detection of IAPP amyloid fibrils. We will continue to modify the probe structure using flavonoid scaffold.

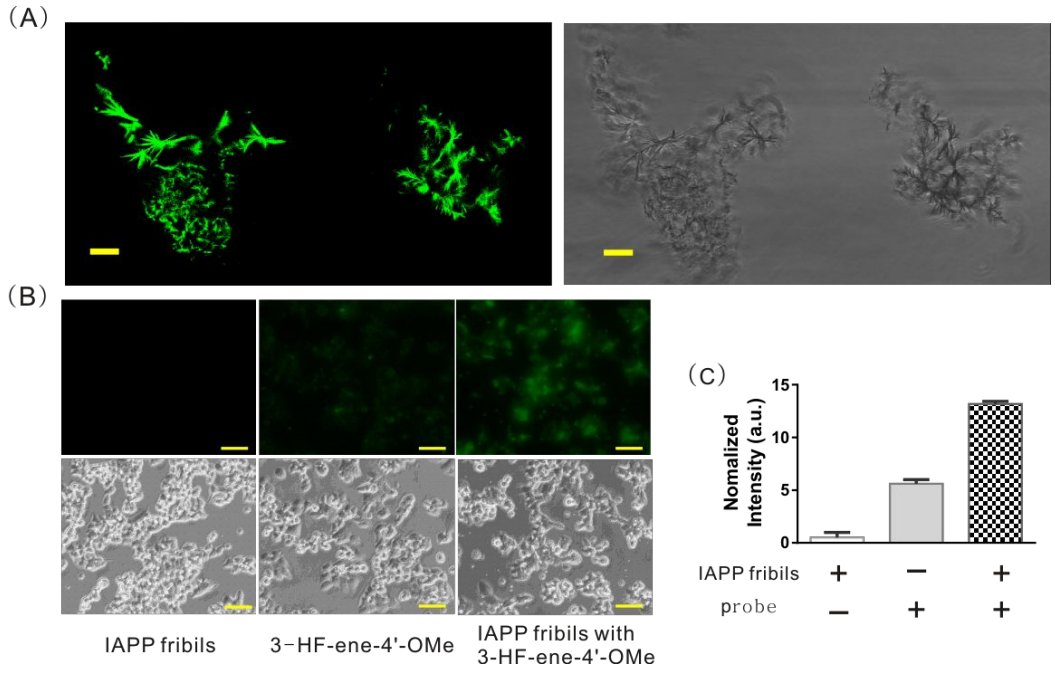

Figure 8. **3-HF-ene-4'-OMe** could detect IAPP fibrils. (A) Confocal microscopy images of **3-HF-ene-4'-OMe** stained IAPP amyloid fibrils. The transmitted light image (right panel) show the presence of IAPP fibrils in targeted area. Fluorescence only can be detected in the area that fibrils are present. The scale bar represents 10 μm (B) Fluorescence images of MIN6 Cells treated with IAPP fibrils (top left panel), with **3-HF-ene-4'-OMe** (top middle panel) and with both (top right panel). Transmitted light images were shown in bottom panels. The scale bar represents 50 μm. (C) The graph shows a quantitative analysis of fluorescence intensity collected from (B).

Conclusions

In the past, several groups were also attempting to detect islet amyloid using fluorescent dye. SYPRO orange was shown to bind IAPP amyloid fibrils with excitation and emission maxima of 490 nm and 594 nm[21]. Our probe can absorb light around 380 nm and fluoresce at about 535 nm upon binding to IAPP fibrils. Besides ThT, these two probes can become useful alternative to monitor IAPP aggregation when a putative inhibitor may interfere ThT spectrum. Stevens and Bourgault groups both have utilized the biarsenical dye, FlAsH, to detect the early stage of IAPP aggregation because FlAsH can recognize tetracysteine motifs from IAPP N-terminal assembly[19, 20]. It would be useful to detect IAPP oligomers using FlAsH. However, its application in cell imaging have not been tested yet. In this study, the flavonoid scaffold was shown to be successfully employed in the design of environmentally sensitive fluorescent probes for the detection of IAPP amyloid fibrils. **3-HF-ene-4'-OMe** gave the largest enhancement of fluorescence intensity upon binding to IAPP fibrils. The conjugated double bonds system seem to make the behavior of the probes as molecular rotor dyes which are sensitive to the environment, as well as to viscosity. We speculate that the conformational flexibility of **3-HF-ene-4'-OMe** is restricted when it binds to the IAPP fibrils and that could significantly contribute to the emission enhancement. In addition, **3-HF-ene-4'-OMe** was more suitable to be used in resveratrol inhibition assay compared with conventionally used ThT. We also demonstrated that non-cytotoxic **3-HF-ene-4'-OMe** was able to detect IAPP aggregates in live cells, but further modification is needed to reduce nonspecific binding to cell membrane. Most importantly, **3-HF-ene-4'-OMe** showed selectivity for detection of islet amyloid as it did not give significant fluorescent signal upon mixing with hCT fibrils or displayed a weaker fluorescent emission with a large blue-shift (70 nm) upon binding to $A\beta_{42}$ fibrils. The different emission profiles, as revealed by molecular docking calculation, might due to the polarity of the binding environment of **3-HF-ene-4'-OMe**. Although it is not able to completely distinguish IAPP and $A\beta_{42}$ fibrils in practical, we believe that use of flavonoid as a molecule scaffold holds potential to develop a specific dye for detection of islet amyloid in T2D.

Supporting Information

Characterization data of all flavonoid-based small molecules and all 1H and 13C NMR data.

Additional experimental details, fluorescence spectra, CD spectra, TEM images, docking analysis and data for cytotoxicity tests.

Author contribution

W. Chen, S. Ma, Y.Chen, Y. Chao, and A. Chan conducted the experiments. L. Tu and W. Liu designed the concept, analyzed the data, and wrote the manucript.

Acknowledgments

This work is financially supported by the Ministry of Science and Technology, Taiwan (project numbers: MOST105-2113-M-030-010-MY2, MOST105-2113-M-003-014-MY2, and MOST106-2320-B-006-058-MY3), the Department of Chemistry, Fu Jen Catholic University, the Department of Chemistry, National Taiwan Normal University and the Department of Pharmacology, College of Medicine, National Cheng Kung University. Special thanks to Prof. Robert Tycko and Prof. Daniel P. Raleigh who kindly provide us the model of IAPP fibrils. We also thank Mr. Yu-Jen Chang for providing technical support in taking confocal fluorescence images.

References

[1] Knowles, T. P. J., Vendruscolo, M., and Dobson, C. M. (2014) The amyloid state and its association with protein misfolding diseases, *Nat. Rev. Mol. Cell Biol. 15*, 384-396.

[2] Chiti, F., and Dobson, C. M. (2006) Protein misfolding, functional amyloid, and human disease, *Annu. Rev. Biochem. 75*, 333-366.

[3] Naiki, H., Higuchi, K., Hosokawa, M., and Takeda, T. (1989) Fluorometric determination of amyloid fibrils in vitro using the fluorescent dye, thioflavin T1, *Anal. Biochem. 177*, 244-249.

[4] LeVine, H., 3rd. (1997) Stopped-flow kinetics reveal multiple phases of thioflavin T binding to Alzheimer beta (1-40) amyloid fibrils, *Arch. Biochem. Biophys. 342*, 306-316.

[5] Sen, P., Fatima, S., Ahmad, B., and Khan, R. H. (2009) Interactions of thioflavin T with serum albumins: Spectroscopic analyses, *Spectrochim. Acta, Part A 74*, 94-99.

[6] Nilsson, M. R. (2004) Techniques to study amyloid fibril formation in vitro, *Methods 34*, 151-160.

[7] Younan, N. D., and Viles, J. H. (2015) A comparison of tree forophores for the dtection of amyloid fibers and prefibrillar oligomeric assemblies. ThT (Thioflavin T); ANS (1-Anilinonaphthalene-8-sulfonic Acid); and bisANS (4,4'-Dianilino-1,1'-binaphthyl-5,5'-disulfonic Acid), *Biochemistry 54*, 4297-4306.

[8] Smith, N. W., Alonso, A., Brown, C. M., and Dzyuba, S. V. (2010) Triazole-containing BODIPY dyes as novel fluorescent probes for soluble oligomers of amyloid Abeta1-42 peptide, *Biochem. Biophys. Res. Commun. 391*, 1455-1458.

[9] Wang, C., Yang, A., Li, X., Li, D., Zhang, M., Du, H., Li, C., Guo, Y., Mao, X., Dong, M., Besenbacher, F., Yang, Y., and Wang, C. (2012) Observation of molecular inhibition and binding structures of amyloid peptides, *Nanoscale 4*, 1895-1909.

[10] Ono, M., Doi, Y., Watanabe, H., Ihara, M., Ozaki, A., and Saji, H. (2016) Structure-activity relationships of radioiodinated diphenyl derivatives with different conjugated double bonds as ligands for [small alpha]-synuclein aggregates, *RSC Adv. 6*, 44305-44312.

[11] Rajasekhar, K., Narayanaswamy, N., Murugan, N. A., Kuang, G., Ågren, H., and Govindaraju, T. (2016) A high affinity red fluorescence and colorimetric probe for amyloid β aggregates, *Sci. Rep. 6*, 23668-23677.

[12] Seo, Y., Park, K. S., Ha, T., Kim, M. K., Hwang, Y. J., Lee, J., Ryu, H., Choo, H., and Chong, Y. (2016) A smart near-infrared fluorescence probe for selective detection of Tau fibrils in Alzheimer's disease, *ACS Chem. Neurosci. 7*, 1474-1481.

[13] Rajasekhar, K., Narayanaswamy, N., Murugan, N. A., Viccaro, K., Lee, H. G., Shah, K., and Govindaraju, T. (2017) Abeta plaque-selective NIR fluorescence probe to differentiate Alzheimer's disease from tauopathies, *Biosens. Bioelectron. 98*, 54-61.

[14] Park, K. S., Yoo, K., Kim, M. K., Jung, W., Choi, Y. K., and Chong, Y. (2017) A novel probe with a chlorinated alpha-cyanoacetophenone acceptor moiety shows near-infrared fluorescence specific for Tau fibrils, *Chem. Pharm. Bull. 65*, 1113-1116.

[15] Klingstedt, T., Shirani, H., Mahler, J., Wegenast-Braun, B. M., Nystrom, S., Goedert, M., Jucker, M., and Nilsson, K. P. (2015) Distinct spacing between anionic groups: An essential chemical determinant for achieving thiophene-based ligands to distinguish beta-amyloid or Tau polymorphic aggregates, *Chem. Eur. J. 21*, 9072-9082.

[16] Cao, K., Farahi, M., Dakanali, M., Chang, W. M., Sigurdson, C. J., Theodorakis, E. A., and Yang, J. (2012) Aminonaphthalene 2-cyanoacrylate (ANCA) probes fluorescently discriminate between amyloid-beta and prion plaques in brain, *J. Am. Chem. Soc. 134*, 17338-17341.

[17] Lv, G., Cui, B., Lan, H., Wen, Y., Sun, A., and Yi, T. (2015) Diarylethene based fluorescent switchable probes for the detection of amyloid-beta pathology in Alzheimer's disease, *Chem. Commun. 51*, 125-128.

[18] Lee, M., Kim, M., Tikum, A. F., Lee, H. J., Thamilarasan, V., Lim, M. H., and Kim, J. (2019) A near-infrared fluorescent probe for amyloid-β aggregates, *Dyes Pigm. 162*, 97-103.

[19] Wang, S.-T., Lin, Y., Hsu, C.-C., Amdursky, N., Spicer, C. D., and Stevens, M. M. (2017) Probing amylin fibrillation at an early stage via a tetracysteine-recognising fluorophore, *Talanta 173*, 44-50.

[20] Quittot, N., Sebastiao, M., Al-Halifa, S., and Bourgault, S. (2018) Kinetic and conformational insights into islet amyloid polypeptide self-assembly using a biarsenical fluorogenic probe, *Bioconjugate Chemistry 29*, 517-527.

[21] Wong, A. G., and Raleigh, D. P. (2016) The dye SYPRO orange binds to amylin amyloid fibrils but not pre-fibrillar intermediates, *Protein Sci. 25*, 1834-1840.

[22] Raleigh, D., Zhang, X., Hastoy, B., and Clark, A. (2017) The beta-cell assassin: IAPP cytotoxicity, *J. Mol. Endocrinol. 59*, R121-R140.

[23] Westermark, P., Andersson, A., and Westermark, G. T. (2011) Islet amyloid polypeptide, islet amyloid, and diabetes mellitus, *Physiol. Rev. 91*, 795-826.

[24] Ping, C., Peter, M., Harris, N., Vadim, P., Ling-Hsien, T., Hui, W., Andisheh, A., and P., R. D. (2013) Islet amyloid: From fundamental biophysics to mechanisms of cytotoxicity, *FEBS Letters 587*, 1106-1118.

[25] Rodriguez Camargo, D. C., Garg, D., Buday, K., Franko, A., Rodriguez Camargo, A., Schmidt, F., Cox, S. J., Suladze, S., Haslbeck, M., Mideksa, Y. G., Gemmecker, G., Aichler, M., Mettenleiter, G., Schulz, M., Walch, A. K., Hrabe de Angelis, M., Feige, M. J., Sierra, C. A., Conrad, M., Tripsianes, K., Ramamoorthy, A., and Reif, B. (2018) hIAPP forms toxic oligomers in plasma, *Chem. Commun. 54*, 5426-5429.

[26] Marsh, D. T., Das, S., Ridell, J., and Smid, S. D. (2017) Structure-activity relationships for flavone interactions with amyloid beta reveal a novel anti-aggregatory and neuroprotective effect of 2',3',4'-trihydroxyflavone (2-D08), *Bioorg. Med. Chem. 25*, 3827-3834.

[27] Bu, X. L., Rao, P. P. N., and Wang, Y. J. (2016) Anti-amyloid aggregation activity of natural compounds: Implications for Alzheimer's drug discovery, *Mol. Neurobiol. 53*, 3565-3575.

[28] Young, L. M., Saunders, J. C., Mahood, R. A., Revill, C. H., Foster, R. J., Tu, L.-H., Raleigh, D. P., Radford, S. E., and Ashcroft, A. E. (2015) Screening and classifying small-molecule inhibitors of amyloid formation using ion mobility spectrometry–mass spectrometry, *Nat. Chem. 7*, 73-81.

[29] Klymchenko, A. S. (2017) Solvatochromic and fluorogenic dyes as environment-sensitive probes: Design and biological applications, *Acc. Chem. Res. 50*, 366-375.

[30] Klymchenko, A. S., and Demchenko, A. P. (2003) Multiparametric probing of intermolecular interactions with fluorescent dye exhibiting excited state intramolecular proton transfer, *Phys. Chem. Chem. Phys. 5*, 461-468.

[31] Chou, P.-T., Yu, W.-S., Cheng, Y.-M., Pu, S.-C., Yu, Y.-C., Lin, Y.-C., Huang, and Chen, C.-T. (2004) Solvent-polarity tuning excited-state charge coupled proton-transfer reaction in p-N,N-ditolylaminosalicylaldehydes, *J. Phys. Chem. A 108*, 6487-6498.

[32] Chen, C. Y., and Chen, C. T. (2013) Reaction-based and single fluorescent emitter decorated ratiometric nanoprobe to detect hydrogen peroxide, *Chem. Eur. J. 19*, 16050-16057.

[33] Basu, S., Mondal, S., and Mandal, D. (2010) Proton transfer reactions in nanoscopic polar domains: 3-hydroxyflavone in AOT reverse micelles, *J. Chem. Phys. 132*, 034701.

[34] M'Baye, G., Klymchenko, A. S., Yushchenko, D. A., Shvadchak, V. V., Ozturk, T., Mely, Y., and Duportail, G. (2007) Fluorescent dyes undergoing intramolecular proton transfer with improved sensitivity to surface charge in lipid bilayers, *Photochem. Photobiol. Sci. 6*, 71-76.

[35] Celej, M. S., Caarls, W., Demchenko, A. P., and Jovin, T. M. (2009) A triple-emission fluorescent probe reveals distinctive amyloid fibrillar polymorphism of wild-type alpha-synuclein and its familial Parkinson's disease mutants, *Biochemistry 48*, 7465-7472.

[36] Yushchenko, D. A., Fauerbach, J. A., Thirunavukkuarasu, S., Jares-Erijman, E. A., and Jovin, T. M. (2010) Fluorescent ratiometric MFC probe sensitive to early stages of alpha-synuclein aggregation, *J. Am. Chem. Soc. 132*, 7860-7861.

[37] Kung, H. F., Lee, C. W., Zhuang, Z. P., Kung, M. P., Hou, C., and Plossl, K. (2001) Novel stilbenes as probes for amyloid plaques, *J. Am. Chem. Soc. 123*, 12740-12741.

[38] Dias, T. A., Duarte, C. L., Lima, C. F., Proença, M. F., and Pereira-Wilson, C. (2013) Superior anticancer activity of halogenated chalcones and flavonols over the natural flavonol quercetin, *Eur. J. Med. Chem. 65*, 500-510.

[39] Arakawa, T. (2018) Acetonitrile as solvent for protein interaction analysis, *International Journal of Biological Macromolecules 114*, 728-732.

[40] Morris, G. M., Huey, R., Lindstrom, W., Sanner, M. F., Belew, R. K., Goodsell, D. S., and Olson, A. J. (2009) AutoDock4 and AutoDockTools4: Automated docking with selective receptor flexibility, *J. Comput. Chem. 30*, 2785-2791.

[41] Xiao, Y., Ma, B., McElheny, D., Parthasarathy, S., Long, F., Hoshi, M., Nussinov, R., and Ishii, Y. (2015) Abeta(1-42) fibril structure illuminates self-recognition and replication of amyloid in Alzheimer's disease, *Nat. Struct. Mol. Biol. 22*, 499-505.

[42] Luca, S., Yau, W. M., Leapman, R., and Tycko, R. (2007) Peptide conformation and supramolecular organization in amylin fibrils: constraints from solid-state

NMR, *Biochemistry 46*, 13505-13522.

[43] Becke, A. D. (1988) Density-functional exchange-energy approximation with correct asymptotic behavior, *Phys. Rev. A 38*, 3098-3100.

[44] Lee, C., Yang, W., and Parr, R. G. (1988) Development of the Colle-Salvetti correlation-energy formula into a functional of the electron density, *Phys. Rev. B 37*, 785-789.

[45] Chang, H. Y., Chen, S. L., Shen, M. R., Kung, M. L., Chuang, L. M., and Chen, Y. W. (2017) Selective serotonin reuptake inhibitor, fluoxetine, impairs E-cadherin-mediated cell adhesion and alters calcium homeostasis in pancreatic beta cells, *Sci. Rep. 7*, 3515-3527.

[46] An, P., Xu, N.-S., Zhang, H.-L., Cao, X.-P., Shi, Z.-F., and Wen, W. (2015) Facile preparation of α-Cyano-α,ω-Diaryloligovinylenes: A new class of color-tunable solid emitters, *Chem. Asian J. 10*, 1959-1966.

[47] Desideri, N., Mastromarino, P., and Conti, C. (2003) Synthesis and evaluation of antirhinovirus activity of 3-hydroxy and 3-methoxy 2-styrylchromones, *Antivir. Chem. Chemother. 14*, 195-203.

[48] Mishra, R., Sellin, D., Radovan, D., Gohlke, A., and Winter, R. (2009) Inhibiting islet amyloid polypeptide fibril formation by the red wine compound resveratrol, *ChemBioChem 10*, 445-449.

[49] Evers, F., Jeworrek, C., Tiemeyer, S., Weise, K., Sellin, D., Paulus, M., Struth, B., Tolan, M., and Winter, R. (2009) Elucidating the mechanism of lipid membrane-induced IAPP fibrillogenesis and its inhibition by the red wine compound resveratrol: a synchrotron X-ray reflectivity study, *J. Am. Chem. Soc. 131*, 9516-9521.

[50] Radovan, D., Opitz, N., and Winter, R. (2009) Fluorescence microscopy studies on islet amyloid polypeptide fibrillation at heterogeneous and cellular membrane interfaces and its inhibition by resveratrol, *FEBS Lett. 583*, 1439-1445.

[51] Tu, L. H., Young, L. M., Wong, A. G., Ashcroft, A. E., Radford, S. E., and Raleigh, D. P. (2015) Mutational analysis of the ability of resveratrol to inhibit amyloid formation by islet amyloid polypeptide: critical evaluation of the importance of aromatic-inhibitor and histidine-inhibitor interactions, *Biochemistry 54*, 666-676.

[52] Braidy, N., Jugder, B. E., Poljak, A., Jayasena, T., Mansour, H., Nabavi, S. M., Sachdev, P., and Grant, R. (2016) Resveratrol as a potential therapeutic candidate for the treatment and management of Alzheimer's disease, *Curr. Top. Med. Chem. 16*, 1951-1960.

[53] Nedumpully-Govindan, P., Kakinen, A., Pilkington, E. H., Davis, T. P., Chun Ke,

P., and Ding, F. (2016) Stabilizing off-pathway oligomers by polyphenol aanoassemblies for IAPP aggregation inhibition, *Sci Rep 6*, 19463.

[54] Postupalenko, V. Y., Shvadchak, V. V., Duportail, G., Pivovarenko, V. G., Klymchenko, A. S., and Mely, Y. (2011) Monitoring membrane binding and insertion of peptides by two-color fluorescent label, *Biochim Biophys Acta 1808*, 424-432.

For Table of Contents Use Only

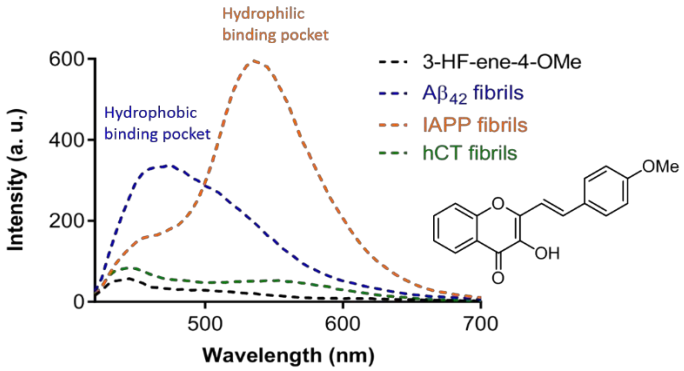

An environmentally sensitive non-cytotoxic probe with flavonoid structural feature is used for detection of IAPP fibrils.